Thermochimica Acta, 91 (1985) 249–263
Elsevier Science Publishers B.V., Amsterdam – Printed in The Netherlands

IRON COMPOUNDS IN HIGH OXIDATION STATES. I. THE REACTION BETWEEN BaO_2 AND $FeSO_4$

E. MARTINEZ-TAMAYO, A. BELTRÁN-PORTER and D. BELTRÁN-PORTER

Departamento de Química Inorgánica, Facultad de Ciencias Químicas, Universidad Literaria de Valencia, Burjassot, Valencia (Spain)

(Received 25 March 1985)

ABSTRACT

The dry methods of preparation of higly oxidized iron compounds usually involve extreme P_{O_2} and T conditions. It seems possible to devise new ways of synthesis in milder conditions. With this purpose, we have approached the study of the role of BaO_2 as the oxidizing agent towards $FeSO_4$ which can act as a precursor of reactive iron oxides. The results described in the present paper show that this reaction enables definite Fe(IV) compounds to be obtained. The ultimate behaviour of the system depends on the ratio between the initial amounts of reagents. The existence of two different ways for the formation of orthoferrate is established.

INTRODUCTION

The existence of compounds containing iron in high oxidation states was known long ago. These compounds, commonly named ferrates, have found a diversity of applications of technological interest (see, e.g., refs. 1–4).

A review of the literature dealing with the preparative procedures of these ferrates shows the existence at present of two essential types of synthetic pathways. The first one implies the oxidation of Fe(III) in a very strong alkaline medium and the subsequent isolation of ferrates(VI) which, in turn, can be used as raw materials for the synthesis of lower ferrates. The second type includes the solid-state ceramic procedures that involve extreme conditions of temperature and O_2 pressure.

We are interested in the reactions occurring in the solid state and our generic goal lies on the design of alternative synthetic ways such that (1) the use of extreme p_{O_2} and T becomes unnecessary and (2) allow the time in which the reactions occur to be relatively shortened. In this way it would also be possible to approach the study of the reaction mechnisms more accurately. Therefore, the influence of several factors contributing to the stabilization of highly oxidized iron could be better understood.

In this context, we have studied the reactions between anhydrous $FeSO_4$ and alkaline or alkaline earth peroxides [5]. The sulphate is a very reactive

0040-6031/85/$03.30

precursor of Fe(III) oxide [6]. The peroxides may act as a source of cations at the same time as being powerful oxidants which are able to replace O_2 gas advantageously. The peroxides, as well as ferrous sulphate, are among the most widely used inorganic industrial chemicals.

In the present paper we describe the phenomenological behaviour of the BaO_2–$FeSO_4$ system. To the best of our knowledge, the literature does not contain any information about it.

As it will be seen later, the main products of reaction for this system (under variable conditions) are Fe(IV) derivatives (having perovskite or related structures). This result should not be very surprising. In practice, the oxidation degree reached by iron in solid-state reactions depends not only on the oxidant agent and working temperature but also largely on the nature of the counter-ion present (as well as, in some cases, on the relationship between the starting amounts of the reagents). Thus e.g., the reaction between Fe_2O_3 and K_2O yields, at 450°C and $p_{O_2} = 1$ atm, III, V or VI ferrates as a function of the initial K/Fe ratio. However, for the Fe_2O_3–BaO system, an analogous variation of the Ba/Fe ratio allows only several tetravalent iron ferrates to be obtained [7].

The following scheme summarizes the methods described for the ferrates(IV) preparation [8]

$$Fe_2O_3 + 2\,BaO \xrightarrow{N_2,\ 1100\text{–}1400^\circ C} 2\,BaFeO_{2.5}$$

$$2\,BaFeO_{2.5} \xrightarrow{\uparrow p_{O_2}T = 7000\ \text{atm}\ ^\circ C} 2\,BaFeO_{2.95}$$

$$Ba_3FeO_5 \quad Ba_2FeO_4$$

$$\uparrow_{x=2} \qquad \uparrow_{x=1}^{p_{O_2}\ 1\ \text{atm},\ 800^\circ C}$$

$$Ba_3[Fe(OH)_6]_2 + x\,Ba(OH)_2;\ [Fe_2O_3 + (3+x)BaO]$$

In general, it can be assumed that the formation of ferrates(IV) involves the reaction between the pyrolysis products of the departure materials (which are likely to be highly reactive oxides generated in situ) and the ulterior oxidation of iron at a T value close to 800°C.

The essential aim of the present paper lies in the elucidation of the relative importance of the variables that govern the synthesis of Ba ferrates(IV). The working conditions and the utilization of BaO_2 as oxidant (and as cation source) guarantee the existence of a negligible value of p_{O_2} in the system.

EXPERIMENTAL

Anhydrous $FeSO_4$ was prepared by dehydration of $FeSO_4 \cdot 7\ H_2O$. This hydrate had been previously recrystallized from analytical grade reagent solutions. Dehydration was carried out at 450°C under a dynamic, dry CO_2

atmosphere. The resulting product was characterized by X-ray powder diffraction [9] and its iron content determined by atomic absorption spectroscopy (exp.: 36.5%; calcd.: 36.78%). The BaO_2 was UCB analytical grade.

To make the samples, the required amounts of both reagents were mixed, ground and homogenized in a Fritch-Pulverisette for 40 min using dry acetone as dispersive medium. The acetone was then removed by heating the samples in a tubular furnace at 150°C while dry N_2 was flowing. The samples were stored in sealed flasks in a desiccator over anhydrous $CaCl_2$.

To follow the reactions occurring between $FeSO_4$ and BaO_2, thermal analysis was utilized. The products originated at the different reaction stages were chemically analysed and characterized by X-ray powder diffraction and IR spectroscopy.

The thermal analyses were made using a Setaram 870 simultaneous TG–DTA thermobalance. Crucibles containing 100 mg of sample were heated at 2.5°C min^{-1} under a dynamic N_2 atmosphere. Calcined Al_2O_3 was used as reference. Calorimetric measurements were performed using a Perking-Elmer 31 DSC.

X-ray powder diffraction patterns were obtained by means of a Kristalloflex 810 Siemens diffractometer using Cu $K\alpha$ radiation. JCPDF cards were utilized as comparative standards.

Infrared spectra (KBr pellet) were recorded with a Pye-Unicam SP2000 spectrophotometer.

Ba was determined gravimetrically as $BaSO_4$. Fe analyses were performed using a Perkin-Elmer 300 AA spectrophotometer. The Fe(IV) content was evaluated by the Mori procedure [10].

SO_2 and SO_3 were identified, after absorption by an alkaline solution, using acid fuchsin [11a] and sodium rhodizonate [11b], respectively.

RESULTS AND DISCUSSION

To elucidate the nature of the reaction, a series of ten samples containing $BaO_2/FeSO_4$ at ratios ranging from 0.50 to 4.00 was prepared. The data set provided by the thermal analysis of these samples has been summarized in Table 1. The respective TG and DTA curves are shown in Fig. 1. Table 2 includes the identified (chemically and/or spectroscopically) chemical species stable at various stages of the reaction processes.

The existence of two thermal effects can be noted at 130 (ENDO) and 370°C (EXO) that look similar in all cases. The first, endothermic peak must be associated with the evolution of the moisture traces absorbed during the handling of the very hygroscopic, anhydrous $FeSO_4$ [9]. (Thus, samples containing only "anhydrous" $FeSO_4$ show, after an analogous handling, a similar endothermic effect. On the other hand, it must be remembered that the samples were dried at 150°C, that is to say, at a temperature higher than

TABLE 1

Thermal analysis data

Sample	Ba/Fe [a]	Thermal effects								
I	0.50	TG [b]	–	1.90			18.79			
		DTA [c]	130↑	370↓			625–715↑			
II	1.00	TG [b]	–	3.00			8.27			
		DTA [c]	130↑	370↓			625–715↑			
III	1.50	TG [b]	–	3.59			2.30			
		DTA [c]	130↑	370↓			625–715↑			
IV	1.75	TG [b]	–	4.18			1.14			
		DTA [c]	130↑	370↓			625–715↑			
V	1.90	TG [b]	–	3.06			0.99			
		DTA [c]	130↑	370↓			625–715↑			
VI	2.00	TG [b]	–	3.03						
		DTA [c]	130↑	370↓						
VII	2.50	TG [b]	–	2.12	1.94					
		DTA [c]	130↑	370↓	395–422↓					
VIII	3.00	TG [b]	–	1.90	2.20	0.79				
		DTA [c]	130↑	370↓	398–424↓	571↓				
IX	3.50	TG [b]	–	1.48	2.78	0.56		0.57		
		DTA [c]	130↑	370↓	398–424↓	549↓		784↑		
X	4.00	TG [b]			2.85	0.60		0.62		
		DTA [c]	130↑	370↓	398–424↓	597↓		790↑		

↑ ENDO; ↓ EXO.

[a] $BaO_2/FeSO_4$ molar ratio.

[b] Percent weight loss.

[c] Temperature (°C).

that corresponding to the endothermic effect mentioned.) Aside from this, the exothermic effect occurring at 370°C is the only effect that can be observed for the sample having a Ba/Fe ratio equal to 2.00 (sample VI). The curves of the remaining samples (whose Ba/Fe ratios are higher or lower than 2.00) show additional peaks at higher temperatures.

The isolated "stoichiometric reaction" between BaO_2 and $FeSO_4$

As we have just stated, a sample containing two BaO_2 molecules per $FeSO_4$ molecule gives rise only to one exothermic peak (at 370°C). The corresponding process is adequately described by the stoichiometric equation

$$2\ BaO_2 + FeSO_4 \xrightarrow[370°C]{N_2} BaSO_4 + BaFeO_3 + 1/2\ O_2 \qquad \text{(a)}$$

The following points support this hypothesis: (1) the thermogravimetric data; (2) the identification of the reaction products (see Experimental and Table 2); and (3) the absence of reagents in the resulting solid mixture.

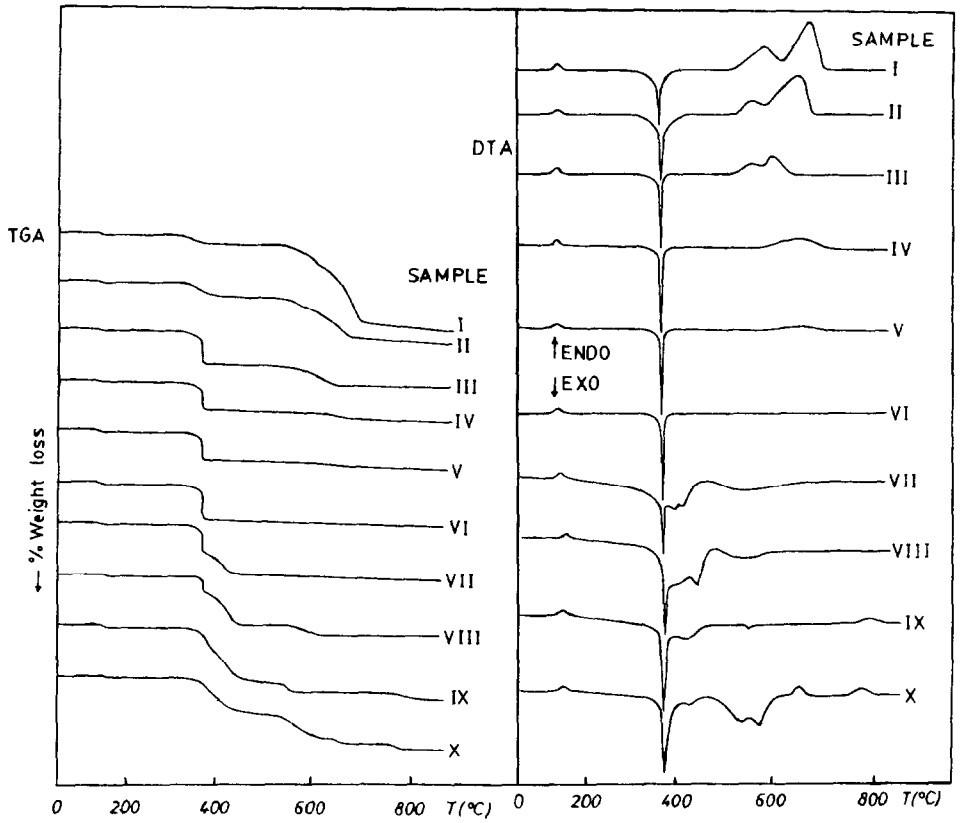

Fig. 1. TG–DTA plots of the samples (dynamic nitrogen atmosphere, 2.5° C min^{-1}).

The cubic perovskite * $BaFeO_3$ (metaferrate IV) is not stable under the working conditions [15] and evolves spontaneously to give a non-stoichiometric triclinic stable phase, $BaFeO_{2.64}$. On heating the sample above 370°C it is evident (TG curve and chemical analysis) that O_2 loss is involved in this transformation. On the other hand, the X-ray diffraction patterns plotted in Fig. 2 show the structural change implied. Thus, the peaks assignable to the perovskite-type compounds appear shifted ** to higher 2θ values in the pattern of the phase formed by air cooling of the 370° reaction mixture to

* All the definite solid phases containing Fe in a high oxidation state identified in this work have the perovskite-type or related structures. Besides the X-ray diffraction patterns of the solids, evidence in this sense has been provided by IR spectroscopy. The strong band at about 825 cm^{-1} (FeO_4^{n-} bending) and the more weak band located at about 320 cm^{-1} (FeO stretching) characteristic of the FeO_4^{n-} regular tetrahedral structural unit [12] are missing in all the recorded spectra. Although Fe is tetracoordinated by four oxygen atoms in the Ba_2FeO_4 phase, the resulting polyhedron must be strongly distorded [13a,14]. This way we can also affirm that only Fe(IV) is originated in these processes.

** The $BaSO_4$ peaks can be used as internal standard.

TABLE 2

Solid and gaseous phases identified at the temperatures indicated

T (°C)	Sample:	I	II	III	IV	VI	VII	VIII
	Ba/Fe:	0.50	1.00	1.50	1.75	2.00	2.50	3.00
375		$BaSO_4$ $FeSO_4$ Fe_2O_3 Fe_3O_4 SO_3	$BaSO_4$ $FeSO_4$ Fe_2O_3 SO_3	$BaSO_4$ $FeSO_4$ Fe_2O_3 SO_3	$BaSO_4$ Fe_2O_3 $BaFeO_{2.64}$ SO_3	$BaSO_4$ $BaFeO_{2.64}$ O_2	$BaSO_4$ $BaFeO_{2.64}$ O_2	$BaSO_4$ $BaFeO_{2.64}$ Ba_2FeO_4 O_2
425		$BaSO_4$ $FeSO_4$ Fe_2O_3 Fe_3O_4 SO_3	$BaSO_4$ $FeSO_4$ Fe_2O_3 SO_3	$BaSO_4$ $FeSO_4$ Fe_2O_3 SO_3	$BaSO_4$ Fe_2O_3 $BaFeO_{2.64}$ SO_3	$BaSO_4$ $BaFeO_{2.64}$ O_2	$BaSO_4$ $BaFeO_{2.64}$ Ba_2FeO_4 O_2	$BaSO_4$ Ba_2FeO_4 O_2
850		$BaSO_4$ Fe_2O_3 SO_2 SO_3	$BaSO_4$ Fe_2O_3 SO_2 SO_3	$BaSO_4$ Fe_2O_3 SO_2 SO_3	$BaSO_4$ Fe_2O_3 $BaFeO_{2.64}$ SO_2 SO_3	$BaSO_4$ $BaFeO_{2.64}$ O_2	$BaSO_4$ $BaFeO_{2.64}$ Ba_2FeO_4 O_2	$BaSO_4$ Ba_2FeO_4 O_2

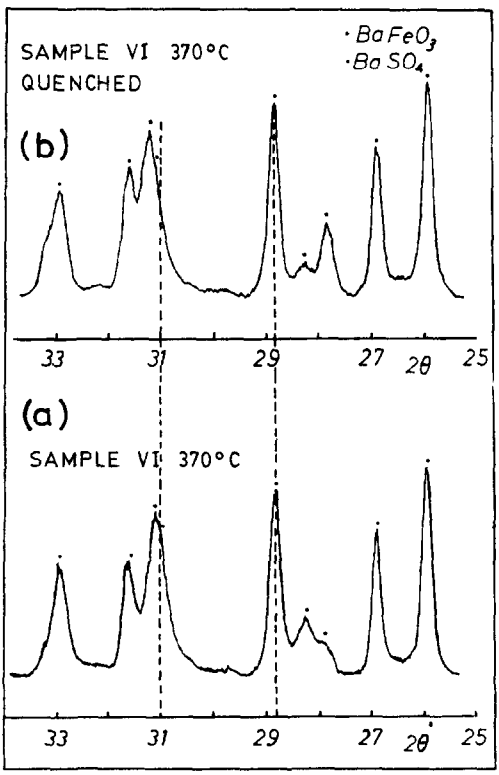

Fig. 2. X-ray powder diffraction patterns of sample VI heated at 375°C: (a) air cooling; (b) quenched into solid CO_2. ($BaSO_4$ peaks were taken as internal standards.)

room temperature (Fig. 2a) with respect to that of the species obtained when the sample is quenched by means of solid CO_2 (Fig. 2b). These phases are unambiguously identifiable as the triclinic $BaFeO_{2.64}$ and the tetragonal $BaFeO_{2.81}$, respectively [15].

According to (1) the characteristic temperature of this first exothermic process (370°C) and (2) the shape of the DTA peak, we can assume that, in all cases, the reaction corresponding to eqn. (a) constitutes the way through which BaO_2 initiates its attack on the anhydrous $FeSO_4$. In this manner, the thermal effects observed at $T > 370$°C can be related to the presence of an excess of $FeSO_4$ (samples I–V) or BaO_2 (samples VII–X) with respect to the stoichiometric amounts (mol BaO_2/mol $FeSO_4 = 2$, sample VI).

Furthermore, as shown in Table 2, $BaSO_4$ is always formed in the process occurring at 370°C but the nature of the additional products obtained depends on the initial Ba/Fe ratio.

Excess of $FeSO_4$

The DTA curves of samples I–V show, in addition to the thermal effects mentioned above at 130 (ENDO) and 370°C (EXO), a complex endothermic effect (peaks at 625 and 715°C) which diminishes smoothly as the Ba/Fe ratio approaches 2.00 (sample VI). Two significant weight losses appear on the TG curves of these samples. The first one is associated with the 370°C process. This weight loss is slow in the case of samples I and II but is rapid (after a short induction period) for samples III–V. The size of the two-step weight loss between 520 and 725°C decreases as we progress through this series, disappearing in sample VI.

There is much evidence supporting the fact that this last two-step process corresponds to the thermal decomposition of anhydrous $FeSO_4$. Thus, we have detected (X-ray powder diffraction) this product among the phases present at 375°C (see Table 2). Likewise, the end product of the pyrolysis was characterized (X-ray powder diffraction) as Fe_2O_3 and the gas evolved during this degradation contains only SO_2 and SO_3 (identified by spot-test analyses). On the other hand, the shape of the TG and DTA curves, as well as the peak temperatures coincide with the literature data [6].

Nevertheless, the amount of $FeSO_4$ involved in this process (calculated from the therogravimetric data) is, in all cases, lower than expected if the reaction described by eqn. (a) was the only one taking place at 370°C. This fact proves the existence of "an excess of $FeSO_4$ comsumption" (with respect to that theoretically calculated according to eqn. (a)) at 370°C, thus suggesting the simultaneous (that is to say, at 370°C) development of side reactions. In Table 3 we have listed the data on $FeSO_4$ comsumption (in the process at 370°C) as a function of the Ba/Fe initial ratios. As it can be noted from the right-hand column of data, the $FeSO_4$ relative consumption comes near to the "stoichiometric" $FeSO_4/BaO_2$ ratio (0.50) along this series as the initial BaO_2 content increases.

TABLE 3

Relative consumption of ferrous sulphate

Sample	Ba/Fe	M_1	M_2	M_3	M_4	M_4/M_2
I	0.50	0.474	0.237	0.138	0.335	1.410
II	1.00	0.333	0.337	0.059	0.278	0.825
III	1.50	0.332	0.498	0.020	0.311	0.626
IV	1.75	0.264	0.462	0.009	0.255	0.552
V	1.90	0.267	0.507	0.008	0.256	0.510
VI	2.00	0.166	0.333	0.000	0.167	0.500

M_1 = initial moles of ferrous sulphate; M_2 = initial moles of barium peroxide; M_3 = moles of ferrous sulphate non-consumed at 370°C; M_4 = moles of ferrous sulphate consumed at 370°C.

The following side reactions in which $FeSO_4$ participates are very likely

$$FeSO_4 + BaFeO_3 \rightarrow BaSO_4 + Fe_2O_3 \quad (b)$$

$$FeSO_4 + Fe_2O_3 \rightarrow Fe_3O_4 + SO_3 \quad (c)$$

where $BaFeO_3$ is the main phase originated by means of reaction (a). The following points support this suggestion: (1) the X-ray powder diffraction patterns of the resulting solid materials show the presence of both iron oxides besides $BaSO_4$ (and, also, $FeSO_4$ (non-consumed) in the samples with lower Ba contents) (see Table 2); and (2) SO_3 is positively identified in the gas evolved. On the other hand, the absence of SO_2 in this gas leaves out the possibility of a simple $FeSO_4$ thermal decomposition as a mechanism for its elimination (This possibility was taken into account in spite of the low temperature of the process (370°C) because its exothermic nature might have caused a local overheating.) Additionally, it has been experimentally observed that the DTA curve of a sample with a molar composition 1 $BaSO_4$/1 $BaFeO_{2.64}$/1 $FeSO_4$ shows a sharp and strong exothermic peak at 370°C, this being consistent with the proposed explanation.

As mentioned above, the weight loss rate at 370°C differs significantly from samples I and II to samples III–V. This fact, that agrees with the proposed scheme (if it is tentatively assumed that reaction (b) goes to completion then reaction (c) only might occur of the samples with a Ba/Fe ratio lower than 1.00; this would lead to the actual existence of different mechanisms depending on the Ba/Fe ratio), suggests that the whole mechanisms of this process are distinct for each one of these sub-series.

Excess of BaO_2

In the case of the samples whose Ba/Fe ratio is higher than 2.00, the DTA curves present a complex exothermic effect (with peaks at ca. 400 and 425°C) overlapping with that at 370°C. The weight loss accompanying this

complex effect is slower than that corresponding to the 370°C step. Samples VIII–X also give rise to additional incidents on DTA and DTG curves at higher temperatures (see Table 1).

The X-ray diffraction pattern of the final solid obtained when sample VIII (Ba/Fe = 3.00) is heated above 650°C shows that the only phase formed is, besides $BaSO_4$, the orthoferrate(IV), Ba_2FeO_4, whose structure might formally be related with that of the perovskite [13a,14].

SO_2 and SO_3 are not present in the gas evolved. The TG data are consistent with the removal of one O_2 mole per each mole of the initial $FeSO_4$, according to the overall reaction

$$3\ BaO_2 + FeSO_4 \rightarrow BaSO_4 + Ba_2FeO_4 + O_2 \uparrow \qquad (d)$$

This total reaction may be regarded as the summation of several consecutive, and partially superimposed, exothermic processes.

As stated above, the attack on $FeSO_4$ by BaO_2 is initiated at 370°C through eqn. (a). The weight loss observed at this temperature indicates that only half of the $FeSO_4$ present reacts at this stage. The perovskite $BaFeO_{2.64}$ is detected when the products of this first reaction are cooled to room temperature. The fact that this last phase is not among the materials yielded at 425°C indicates that the metaferrate and the remaining $FeSO_4$ combine with the unreacted (at 370°C) BaO_2. These last processes would produce the two-step exothermic effect arising between ca. 375 and 430°C. Accordingly, and taking into account the identified products, the following equations can be proposed (the stoichiometric coefficients are referred to the inital amounts of reactants)

First stage (370°C)

$$BaO_2 + 1/2\ FeSO_4 \rightarrow 1/2\ BaSO_4 + 1/2\ BaFeO_3 + 1/4\ O_2 \uparrow \qquad (e)$$

Second stage (375–430°C)

$$1/2\ BaO_2 + 1/2\ BaFeO_3 \rightarrow 1/2\ Ba_2FeO_4 + 1/4\ O_2 \uparrow \qquad (f)$$

$$3/2\ BaO_2 + 1/2\ FeSO_4 \rightarrow 1/2\ BaSO_4 + 1/2\ Ba_2FeO_4 + 1/2\ O_2 \uparrow \qquad (g)$$

This set of reactions implies the existence of two different orthoferrate formation mechanisms. However, it must be said that the experimentally observed weight loss in the second stage is somewhat lower than that expected according to eqns. (f) and (g). This departure will obviously be related to the exothermic process arising at about 570°C which is associated with a new, significant weight loss. It must be emphasized here that the X-ray powder diffraction patterns of samples heated at 450 and 650°C allow the same solid phases to be detected (Ba_2FeO_4 and $BaSO_4$) in both cases. The only remarkable change induced by the rising temperature is an increase in magnitude and a better definition of the peaks assignable to the orthoferrate (Fig. 3), thus suggesting a greater crystallinity of the material at the higher temperature. This fact, and the exothermic character of the process at

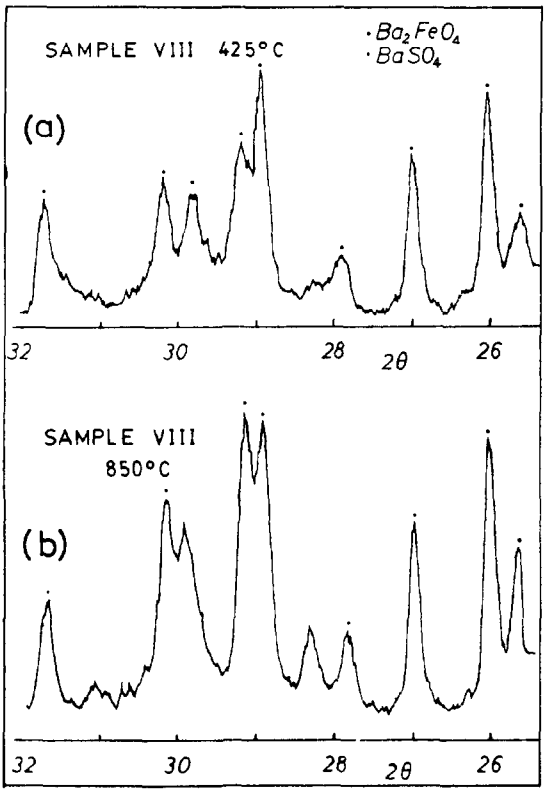

Fig. 3. X-ray powder diffraction patterns of sample VIII heated at (a) 425°C, (b) 850°C.

570°C, should indicate the stabilization of the orthoferrate lattice. The simultaneous weight loss could be understood if it is assumed that O_2^{2-} groups have partially replaced O^{2-} ions. This interpretation, that would also enable us to explain the irregularity mentioned above for the weight loss between 375 and 430°C, finds support in the literature. Thus, $BaO–BaO_2$ solid solutions of variable composition have been reported in detail [16]. On the other hand, given that the atoms are loosely packed in the β-K_2SO_4 type structure of Ba_2FeO_4, there should be sufficient room to accomodate the more bulky O_2^{2-} anions without bringing about a strong structural disturbance. Moreover, the structural relationship between the barium meta- and ortho-ferrates facilitates the understanding of the substitution process. Thus, the structure of Ba_2FeO_4 is closely related to that of Sr_2FeO_4 (K_2NiF_4 [13b]) which, in turn, is derived from the perovskite metaferrate structure by the introduction of a layer of Ba and O ions between double perovskite layers [7].

With respect to sample VII (Ba/Fe = 2.50) the absence of any thermal effect above 430°C must be noted. The total weight loss on heating this sample is compatible with the reaction

$$5/2\ BaO_2 + FeSO_4 \rightarrow BaSO_4 + 1/2\ BaFeO_3 + 1/2\ Ba_2FeO_4 + 3/4\ O_2 \quad (h)$$

where all three solid phases have been identified (X-ray powder diffraction) in the mixture obtained at high temperatures (see Table 2). The weight loss can be separated into two others according to

First stage (370°C, sharp)

$$3/2\ BaO_2 + 3/4\ FeSO_4 \rightarrow 3/4\ BaSO_4 + 3/4\ BaFeO_3 + 3/8\ O_2 \uparrow \quad (i)$$

Second stage (375–430°C, slower)

$$1/4\ BaO_2 + 1/4\ BaFeO_3 \rightarrow 1/4\ Ba_2FeO_4 + 1/8\ O_2 \uparrow \quad (j)$$

$$3/4\ BaO_2 + 1/4 FeSO_4 \rightarrow 1/4\ BaSO_4 + 1/4\ Ba_2FeO_4 + 1/4\ O_2 \uparrow \quad (k)$$

that is to say, a set of reactions parallel to those proposed above for sample VIII. However, in this case, there is no disagreement between the predicted and the observed weight losses and this is consistent with the lack of a thermal effect at ca. 570°C. The process of O_2^{2-} inclusion/elimination is not detected (see Table 2).

In accordance with these results, the existence of two mechanisms of orthoferrate formation can be reaffirmed. Taking into account eqns. (f), (g) and (j), (k) and paying attention to the inversion of the relative intensity of the DTA peaks at ca. 400 and 425°C for samples VIII and VII, it can be established that (1) orthoferrate formation begins with metaferrate formation (370°C), this being immediately followed (ca. 400°C) by its attack by BaO_2, and (2) this first process induces the direct reaction between BaO_2 and $FeSO_4$ (ca. 425°C) also to form Ba_2FeO_4.

We have tried to show semi-quantitatively the relative importance and the temporal sequence (formation degree, α vs. t) of both formation mechanisms by means of Figs. 4a and 4b. Thus, the curves A and B of these plots represent the change in the amounts of $BaFeO_3$ and Ba_2FeO_4, respectively, present in each one of the samples as a function of time (or, which is effectively the same, as a function of T).

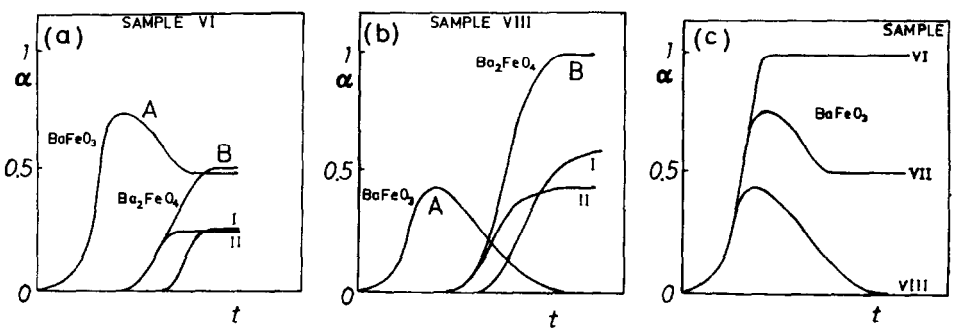

Fig. 4. Relative incidence and temporal sequence of the two different formation mechanism of Ba_2FeO_4 in (a) sample VII and (b) sample VIII. Curves I and II represent, respectively, the direct and the two-step proposed mechanism. (Curves A and B show the formation of meta- and ortho-ferrate, respectively.) (c) Temporal sequence and consumption of barium metaferrate in samples VI, VII and VIII.

Metaferrate formation always precedes the apparition of orthoferrate. Then, it is partially (sample VII) or completely consumed (sample VIII) in the reaction with BaO_2 (see Fig. 4c). The development of this last reaction is indicated by curves II (Figs. 4a and 4b). The direct mechanism (reactions (g) and (k)) has been plotted as curves I.

Dealing with the samples with a high Ba content (Ba/Fe = 3.50 and 4.00; samples IX and X, respectively) the following aspects must be emphasized: (1) as it can be seen in Fig. 1, they have a more complex behaviour than the above-mentioned samples; (2) however, the attack reaction should be, as well as in all the studied cases, represented by eqn. (a) (as suggested by the characteristic exothermic peak at 370°C); (3) notwithstanding, the only well-crystallized phase identified over the whole T range investigated is $BaSO_4$. The remaining solid products were amorphous or poorly crystallized.

These considerations, besides the thermogravimetric data and the experimentally observed extreme reactivity of the obtained solid phases with water, lead us to think about the presence of Fe(V) (see ref. 7) in the materials obtained.

Thermochemical calculations

The variation of enthalpy associated with reaction (a) has been measured by means of DSC. This value and the literature data concerning the formation of products and reagents [17] have allowed us to make the set of approximate thermodynamic calculations assembled in Tables 4 and 5.

In order to calculate the values listed in Table 4 we have kept to the following approach: (1) from the measured ΔH_r (a) values, $\Delta H_f^0(BaFeO_3)$ has been determined assuming that for reaction (a), ΔH_r is not very sensitive towards T; (2) using $\Delta H_f^0(BaFeO_3)$ a Born–Haber cycle allows us to estimate the lattice energy, U, for this phase. The Kapustinskii approximate equation * provides us with a second value for this magnitude, U_K. In this

TABLE 4

Thermodynamic data (kcal mol^{-1})

	$-\Delta H_f^0$	$-U_K$ [a]	$-U$ [b]
$BaFeO_3$	184	3465	3821
$BaFeO_{2.5}$	422	2477	2724
Ba_2FeO_4	527	4408	4849

[a] Lattice energy calculated from Kapustinskii equation.

[b] Lattice energy estimated from thermochemical data.

* An idealized C_xO_y compound has been considered and the size of the "average" cation ($C^{(2y/x)+}$) has been established in such a way that the potential energy per unit cell remains constant. The effective ionic radii data used in the calculations are based on Shannon's work [18].

TABLE 5

Thermodynamic data (kcal mol^{-1})

	ΔH_R	ΔG_R^{634K}
$2\ BaO_2 + FeSO_4 \rightarrow BaSO_4 + BaFeO_3 + H_2O_2$	−5	−37
$3\ BaO_2 + FeSO_4 \rightarrow BaSO_4 + Ba_2FeO_4 + O_2$	−195	−227
$BaO_2 + FeSO_4 \rightarrow Ba_2FeO_4 + 1/2\ O_2$	−190	−206
$BaFeO_3 \rightarrow BaFeO_{2.5} + 1/2\ O_2$	−238	−246

way, a conversion factor may be defined which renders both values coincident; (3) for the remaining phases, the Kapustinskii lattice energy can be corrected using the conversion factor. This "normalized" value leads to the calculated ΔH_f^0 value. From ΔH_f^0 in Table 4, the values in Table 5 are determined. It has been assumed that ΔS_R^0 comes only from the gas evolution.

This collection of data supports the feasibility of both the proposed mechanisms for the reaction between BaO_2 and $FeSO_4$. To sum up, it seems evident that the direct attack reaction can compete with that involving the formation of metaferrate as intermediate. Moreover, the raised reactivity of this last phase becomes manifest as much by its trend to autoreduction (to give the $BaFeO_{2.5}$ perovskite phase *) as by its role as intermediate in the formation of stable orthoferrate.

On the other hand, the good agreement of the calculated U values with those reported in the literature for similar phases must be stressed [19].

CONCLUDING REMARKS

From above, the double function of BaO_2 must be noted: it supplies the required BaO while acting as a suitable oxidizing agent to reach high Fe oxidation states. $FeSO_4$, which certainly is a precursor of iron oxides in the very reactive state, also behaves as an SO_3 "combustible" source. The highly exoenergetic $BaSO_4$ formation reaction becomes the main "thermodynamic motor" of the whole process.

Dealing with the mechanistic aspects (the formal kinetic study of the system has been performed by isothermal and non-isothermal procedures; the results obtained will be reported and discussed in a forthcoming paper) it is worth emphasizing the following considerations: (1) regardless of the

* This Fe(III) phase is the more stable of the barium–iron–perovskite materials. Thus, it does not react with BaO_2 to form orthoferrate. This fact, experimentally checked, agrees with that expected from the data in Tables 4 and 5 which indicate that the mentioned reaction is forbidden at $T < \sim 3900$ K.

composition of the sample, the inital attack implies the formation of metaferrate; (2) this process occurs through direct reaction; (3) the orthoferrate formation proceeds along a double pathway: (a) with metaferrate intermediate apparition which should be analogous to the proposed orthotitanate formation scheme [20], and (b) by direct reaction.

It is remarkable that the Ba cation greatly stabilizes the oxidation state IV even in the presence of a theoretical excess of oxidant. This result confirms the literature data and contrasts with the effects induced by the alkaline cations [7]. The stoichiometric ionic ratio in "ferrates", conditioning the available structure types, is closely related (through the resulting lattice energies) to the stabilization of determined oxidation states. With respect to the barium phases, the perovskite-type structure, allowing the autoreduction by O_2 elimination without change of structural type, should become less stable than the β-K_2SO_4 structure of Ba_2FeO_4 (which lacks a simple reduction route).

Finally, it can be pointed out that the discussed reaction is "adequate" in the obtention of Fe(IV) phases but not clean (it always yields $BaSO_4$ as a side product). Although in line with the results above, the reaction between BaO_2 and FeO will be less advantageous from a thermodynamic viewpoint, it should be a clean reaction. The study of this suggested alternative is now in an advanced stage.

ACKNOWLEDGEMENTS

We thank Dr. T. Rojo from the Euskal Herriko Unibersitatea for the fulfilment of the DSC measurements. Grateful acknowledgement is made to the C.A.I.C.Y.T. for partial support of this research under Grant No. 2930/83.

REFERENCES

1 K.R. Murmen and P.R. Robinson, Water Res., 8 (1974) 543.
2 T. Schink and T.D. Waite, Water Res., 14 (1980) 1705.
3 Standard Oil Development Co., Br., 641, 261, 9-8-1950.
4 G. Peronne, Chal. Ind., 36 (1955) 354.
5 E. Martinez Tamayo, Ph. D. Thesis, Universidad de Valencia, Spain, 1983.
6 P.K. Gallagher, D.W. Johnson and F. Schrey, J. Am. Ceram. Soc., 53 (1970) 666.
7 I.C. Kokarotseva, I.N. Belyaev and L.V. Semenyakova, Russ. Chem. Rev., 41 (1972) 929.
8 E. Martinez Tamayo and D. Beltrán-Porter, in M.T. Clavagera-Mora (Ed.), C.R. 9eme Journée d'Etude des Equilibres entre Phases, Universided de Barcelona, 1983, p. 93.
9 J. Coing-Boyat, Acta Crystallogr., 12 (1959) 939.
10 S. Mori, J. Am. Ceram. Soc., 48 (1965) 165.
11 F. Feigl, Spot Tests in Inorganic Analysis, Elsevier, Amsterdam, 1958, (a) p. 311, (b) p. 313.

12 N. Beraud, Commis. Energ. At. Fr. Rapp., 2895 (1966).
13 A.F. Wells, Structural Inorganic Chemistry, 4th edn., Clarendon Press, Oxford, 1975, (a) p. 946, (b) p. 490.
14 A.J. Bland, Acta Crystallogr., 14 (1961) 875.
15 S. Mori, J. Am. Ceram. Soc., 49 (1966) 600.
16 I.I. Vol'nov, Peroxides, Superoxides and Ozonides of Alkali and Alkaline Earth Metals, Plenum Press, New York, 1966, Chap. 3.
17 (a) Handbook of Chemistry and Physics, 60th edn., C.R.C. Press, Boca Raton, Fl., 1980; (b) M.C. Ball and A.H. Norbury, Physical Data for Inorganic Chemists, Longman, London, 1974; (c) W.E. Dasent, Inorganic Energetics, Penguin Books, Middlessex, U.K., 1970; (d) D.A. Johnson, Some Thermodynamic Aspects of Inorganic Chemistry, Cambridge University Press, London, 1970.
18 R.D. Shannon, Acta Crystallogr., Sect. A, 32 (1976) 751.
19 F.S. Galasso, Structure, Properties and Preparation of Perovskite-Type Compounds, Pergamon Press, Oxford, 1969, p. 39.
20 A. Beauger, J.C. Mutin and J.C. Nrepce, J. Mater. Sci., 18 (1983) 3543.